Pressure measurement at high temperature using ten Sm:YAG fluorescence peaks

Yuechao Zhao, William Barvosa-Carter,[a] Steven D. Theiss,[b] Salman Mitha,[c] and Michael J. Aziz[d]
Division of Engineering and Applied Sciences, Harvard University, Cambridge, Massachusetts 02138

David Schiferl
Los Alamos National Laboratory, Los Alamos, New Mexico 87545

(Received 5 September 1997; accepted for publication 6 July 1998)

A high-temperature pressure calibration technique using Sm-doped $Y_3Al_5O_{12}$ (Sm:YAG) crystal as the pressure calibrant has been developed by studying its Y1 through Y10 fluorescence peaks (frequencies from 15 600 to 17 200 cm^{-1}) at pressures (p) from 1 bar to 19 GPa and temperatures (T) from 20 to 850 °C in externally heated diamond anvil cells. The entire spectrum was fit to a sum of ten Lorentzians plus a linear background. The positions, relative intensities and widths were represented by empirical functions of p and T. Several fitting routines for p determination were created based on these dependences, and were tested on various high-p and high-T experimental Sm:YAG fluorescence spectra. The p values obtained from the fitting routines are compared with those obtained from the ruby and the nitrogen (N_2) vibron pressure scales. A fitting routine is proposed that can determine p from 20 to 850 °C within an estimated uncertainty of 0.4 GPa. © *1998 American Institute of Physics.* [S0021-8979(98)06019-8]

I. INTRODUCTION

Simultaneous high-pressure (p) and high-temperature (T) can be created and adjusted by utilizing the resistively-heated diamond anvil cell (DAC) technique. While measurement of T is straightforward and accurate in this technique, calibration of p is still under development searching for effective, convenient and inert pressure calibrants that are able to work over as large a T and p range as possible. Pressure calibrants fall into mainly two categories: the x-ray diffraction pressure markers and the optical spectroscopic pressure sensors. Some materials such as gold[1] and tungsten[2] with known equations of state may be used over a very wide T regime for p determination by measuring the lattice parameters of these materials using x-ray diffraction. Simultaneous high-p and high-T applications usually require *in situ* control over pressure, and in turn require a pressure measurement technique that can be used to quickly determine p. For quick and accurate p determination, the x-ray diffraction method needs a very strong, well collimated x-ray source, such as synchrotron radiation, which is not available in most laboratories. Moreover, the likelihood that metallic pressure calibrants, which tend to touch the sample during the experiment, may contaminate or be contaminated by the sample at high T further precludes the use of these x-ray pressure calibrants in many experiments, including measurements on diffusion in semiconductor materials[3,4] where an inert and clean environment is vital. For high p work with the DAC, ruby is the most commonly used optical pressure calibrant and the associated spectroscopic pressure calibration method is a standard technique.[5–7] With this technique p can be determined accurately and quickly based on the p and T dependences of the R1 and R2 fluorescence peak wavelengths. However, the intensities of R1 and R2 decrease rapidly with T and become extremely difficult to use above 200 °C, rendering the ruby calibrant of little use in applications involving higher temperatures.

Several other optical pressure calibrants have been proposed and studied for their applications involving high T and high p. These calibrants include Eu:YAG,[8] $Sm:SrB_2O_4$,[9] Sm:SrFCl,[10] N_2,[11] and Sm:YAG.[12–17] Most recently, the diamond $^{13}C/^{12}C$ system was proposed for pressure calibration using the ^{13}C Raman shifts.[18] Among these pressure calibrants, Sm:YAG has the following advantages.

(1) Unlike many other calibrants, the Y1 peak of the Sm:YAG fluorescence has adequate intensity-to-background ratios and can be well resolved even at 700 °C.[12,14,15] Also the cubic phase of YAG remains stable up to 180 GPa.[16,17] Furthermore, while pressure quench of fluorescence is observed in some calibrants such as Sm:SrFCl below 20 GPa,[10] the strongest peaks in Sm:YAG remain strong at high p, and are even an order of magnitude stronger than R1 and R2 signals of ruby above 30 GPa. Thus, the use of Sm:YAG as a pressure calibrant in an extended p and T area is feasible.

(2) The positions of the Y1 and Y2 peaks were found to have negligibly small T dependence,[12,14,15] and thus the p values determined using these two peaks for the pressure scale will be largely insensitive to errors in T measurement. This behavior of Sm:YAG is especially useful for laser heated DAC work, where temperature conditions are usually not known very well.

[a]Present address: Naval Research Laboratory, Washington, D.C. 20375.
[b]Present address: Charles Evans and Associates, 240 Santa Ana Court, Sunnyvale, CA 94063.
[c]Present address: Lawrence Livermore National Laboratory, Livermore, CA 94551.
[d]Electronic mail: maziz@harvard.edu

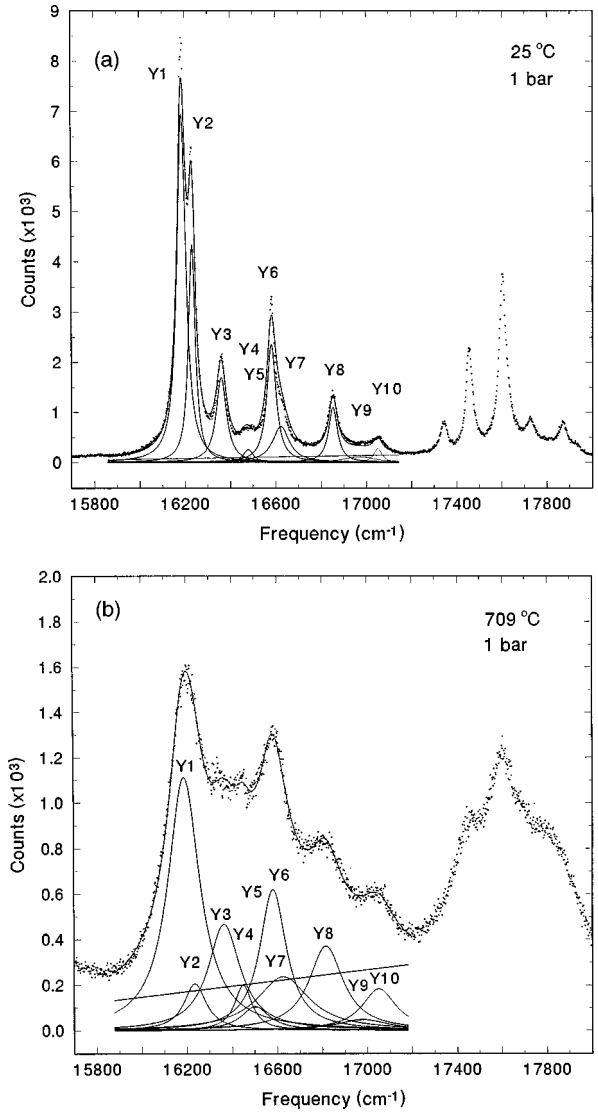

FIG. 1. Sm:YAG spectra at (a) 20 °C and at (b) 709 °C at 1 bar. The individual peak profiles, shown to indicate the interference among Y1 the neighboring peaks, are calculated from the data in Figs. 3–6. Note that in (a), the peak centers are correctly positioned despite the fact that the line shape are approximated by Lorentzians, and complicating factors such as the slit functions are ignored.

(3) Sm:YAG exhibits excellent chemical stability and inertness over a wide T range. This character helps fulfill a clean, inert sample environment during experiments.

(4) Like the measurement technique for ruby fluorescence, the measurement technique for Sm:YAG fluorescence is simple and the optical setup can allow a large amount of free space around the DAC for accommodating other instruments for a specific experiment.

With these advantages, Sm:YAG is therefore one of the best pressure calibrants for applications involving high p and high T. Despite these advantages, however, the use of Sm:YAG has been limited because the peaks of its Y band are close together and overlap even at room T, as shown in Fig. 1. This is in contrast to ruby where R1 and R2 are well isolated, or $Sm:SrB_4O_7$ and Sm:SrFCl, which have singlets. As T increases, the overlapping gets more and more serious due to peak broadening. To take advantage of the high-T characteristics of Sm:YAG, it is necessary to develop a fitting technique that can reliably and precisely resolve these overlapping peaks at as high a T as possible. This is the main purpose of the present study.

Previous studies predominately focused on the p and T behavior of Y1–Y2 doublet.[12–17] Several empirical models have been established in which p is determined using the position of Y1, which is found by fitting three Lorentzian functions plus a linear background to the Y1, Y2, and Y3 peaks. For convenience, this method is hereafter referred to as the Y1–Y3 fitting method. As shown in Fig. 1(b), however, at T above 550 °C these three peaks begin to overlap seriously with the neighboring peaks and the Y3 peak is almost hidden by the background. Thus, the Y1–Y3 method cannot provide accurate and reliable determination of the Y1 position above 550 °C, and therefore it is necessary to take into account as many peaks as possible that overlap and affect Y1. As shown in Fig. 1, nevertheless, interference among the peaks inside the frequency region from Y1 through Y10 (15 800 through 17 200 cm^{-1}) is much more serious than interference coming from any peaks outside this region. We have examined the effect of peaks outside the Y1–Y10 region, i.e., the peaks with frequencies smaller 15 800 cm^{-1} and larger 17 200 cm^{-1}, by extrapolating the tails of the peaks immediately beyond both sides of the Y1–Y10 region as effective pseudo-backgrounds. We found that with and without the extrapolation, the pressure calibration results based on the Y1 scale were essentially identical. We conclude that contributions due to peaks outside Y1–Y10 are negligible and thus we limit our study to the Y1–Y10 frequency range.

In the present study, Sm:YAG spectra with high resolution were acquired at Los Alamos National Laboratory (LANL). These spectra were used to determine p and T dependences of the positions, relative intensities, and widths for the Y1–Y10 peaks. Based on these dependences, we devised several fitting routines for pressure calibration and tested them with various Sm:YAG spectra acquired at both LANL and Harvard, respectively, using the N_2 vibron pressure scale as a reference at some temperatures. We demonstrate fitting routines capable of determining p values that are as accurate and reliable as those from the ruby and the N_2 vibron scales up to 400 °C, and within an estimated uncertainty of 0.4 GPa from 400 to 850 °C.

II. EXPERIMENTAL PROCEDURES

The sample material was the homogenous crystal of $Y_3Al_5O_{12}$ (YAG) doped with 4 wt % Sm, grown by the Czochralski method.[19] Sm:YAG fluorescence spectra were acquired both at LANL and Harvard. The spectra acquired at LANL have higher resolution. Most of the LANL Sm:YAG spectra were acquired under either 20 °C isothermal compression or 1 bar isobaric heating. These higher resolution spectra are used for determining the p and T dependences of the peak parameters of Y1 through Y10. Several of the LANL Sm:YAG spectra were collected under simultaneous high p and T together with N_2 vibron Raman scattering spectra. The N_2 vibron Raman shifts were used for p calibration

based on the scale given by Schmidt *et al.*[11] The Sm:YAG spectra collected at Harvard were used for testing the *p* calibration fitting routines. The spectroscopic detection system at Harvard has not as high a resolution as the system at LANL, but allows for shorter acquisition time. The use of two different laboratories was important for finding a fitting routine for which the *p* values are insensitive to the instrumental setup and parameters.

A. Experiment at LANL

To obtain the *p* and *T* coefficients of the Sm:YAG spectra, a DAC of Merrill–Bassett design was loaded with Sm:YAG and ruby chips, in a pressure medium of liquid argon. To minimize the data acquisition time (especially at high *T*), two SPEX 1403 double-grating spectrometers with 1800 grooves/mm holographic gratings were used to obtain spectra. Photomultiplier tubes were used to detect light, and photon counting electronics were employed. An image of the DAC sample chamber was focused directly onto the slits of one spectrometer, and Raman and fluorescence spectra were excited using the 488 nm line from and argon-ion laser in a nearly backscattering geometry. An image of the back of the sample chamber was focused onto the surface of a polished optical fiber, which transmitted light to the second spectrometer.[20] Using this dual spectrometer configuration, it was possible to simultaneously collect data from two spectral ranges. For the cell loaded with argon, Sm:YAG data were obtained with the first spectrometer, and ruby spectra obtained using the second. Data were obtained at *p* ranging from 1.2 to 20 GPa at room *T*.

Using the furnace described by Zinn *et al.*[21] simultaneous high-*p* and high-*T* spectra were also obtained at ~7 GPa (up to 400 °C and ~14 GPa (up to 700 °C). Three thermocouples were anchored to the DAC, and were observed to read within 2 °C. For measurements of the *T* dependence of the Sm:YAG fluorescence at ambient pressure, a large piece (~0.25 cm^3) of Sm:YAG was clamped between the two plates of a DAC. This was done to have approximately the same thermal mass as a loaded DAC. This cell was then heated in the furnace, and the entire spectral region was obtained for *T* ranging from 20 to 700 °C, in roughly 100 °C increments. To obtain additional simultaneous high-*p* and high-*T* spectra, one of the DACs originally used by Hess and Schiferl[15] was used. The sample chamber was pressurized to ~20 GPa at room *T*, with Sm:YAG, ruby, and a pressure medium of N_2. Because of previous heating of the cell above 400 °C, chemical reaction with the N_2 pressure medium had caused the gasket to weld to the diamond anvil. Using the above method for collecting spectra, we were able to collect the Sm:YAG and N_2 spectra with one spectrometer, and the ruby fluorescence with the other. Spectra were easily obtained for *T* up to 400 °C. Above this *T* the N_2 was observed to melt. Unfortunately, convection caused by local heating from the probe laser caused movement of the Sm:YAG pieces in the cell, and we were unable to collect reliable spectra at higher *T*.

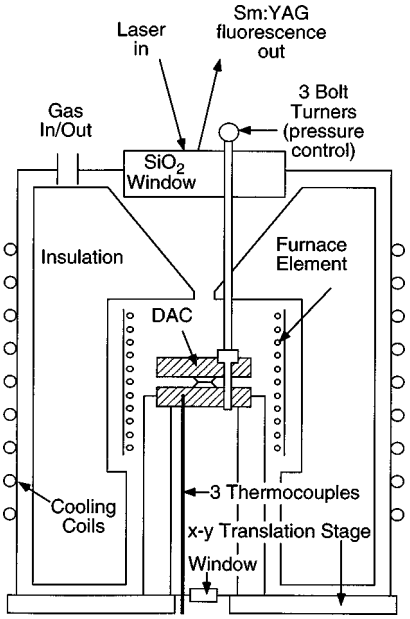

FIG. 2. Schematic of high-temperature and high-pressure system used for the experiments at Harvard.

B. Experiment at Harvard

At Harvard, *p* and *T* were generated using a modified Merrill–Bassett DAC that is externally heated inside the furnace as shown in Fig. 2.

The main body of the DAC was constructed out of Haynes 230® superalloy, which maintains adequate strength and toughness up to 1200 °C. To improve pressure stability at high *T*, the bolts were made out of rhenium, which has a low thermal expansion coefficient. Argon, loaded cryogenically into the DAC from an Ar gas of nominal purity 99.95%, was used as the pressure transmitting medium. Both pure rhenium and molybdenum-50 at. % rhenium alloy were used as gasket materials. Both gasket materials maintain adequate strength even at 850 °C. Alloying of Re with Mo reduces the hardness and brittlness of Re, which not only makes gasket preindentation safe when anvils with large culets ($\geqslant$0.7 mm) were used, but also improves the gasket seal by minimizing the formation of microcracks on the periphery of the gasket hole. While pure Re did not react with the diamond even at 850 °C, Mo–Re was observed to interact with the diamonds at above 800 °C as evidenced by some small pits on the gasket-contacting area of the anvils. Polishing the surface of the Mo–Re sheet before use as a gasket helped reduce the amount of the pits but did not eliminate them. The formation of these features may be caused by (inter)diffusion bonding and/or some kind of chemical reaction. The initial gasket thickness was 250 μm. When using Re, the gasket was first indented to about 120 μm, and then a 280 μm hole was drilled. The gasket was then indented to a final thickness between 50 and 70 μm. The final gasket hole was enlarged to 380 μm in diameter. Mo–Re gasket could be indented in one step all the way down to a thickness between 50 and 70 μm without risking of damage to anvils as long as the indentation proceeds slowly. The hole of the Mo–Re gaskets was also drilled to 380 μm in diameter.

Prior to heating, the furnace was evacuated and then filled with helium gas of nominal purity 99.995% with an overpressure of 260 Torr. The He ambient provides a homogenous temperature field around the DAC and minimizes oxidation of everything inside the furnace. Pressure in the DAC can be controlled from outside the furnace without disturbing the vacuum or the overpressure state in the furnace. The temperature was controlled using a programmable Eurotherm 818 temperature controller. Three thermocouples, two in contact respectively to the upper and the lower plates, and one placed in between the plates, were used to measure *T*. The variation among these thermocouple readings is within 3 °C. The reported *T* value is taken as an average value of the three thermocouple readings. The thermocouples were calibrated using the 1 bar melting points of Pb (328 °C), Sb (631 °C), GaSb (710 °C), NaCl (810 °C), and Ag (961 °C). The melting points were reproduced within ±10 °C.

Sm:YAG chips smaller than 5 μm in size were loaded in the DAC sample chamber. The Sm:YAG fluorescence was excited using the 488 nm line from an argon ion laser (Coherent Innova 70) and detected using a 170° backscattering geometry by an intensified 1024 channel photodiode-array detector (EG&G 1462) mated with a 0.25 m focal length spectrograph (Aries FF250) with a 120 grooves/mm grating. The width of the entrance slit of the spectrograph was typically set to 80 μm. With this width for the entrance slit, the resolution of the detection system was approximately 6 cm^{-1}, which is lower than that obtained at the LANL. Resolution can be made slightly better by narrowing the entrance slit to as small as 25 μm, which is the pixel size of the diode-array detector, and by using longer spectrum acquisition times to obtain the necessary signal-to-noise ratio. For simultaneous high-*p* and high-*T* experiments, especially for those requiring a stable pressure, long acquisition time is problematic because the pressure needs to be tracked quickly, and a balance between resolution and acquisition time must be made. Fortunately, it will be shown that the routines demonstrated here still can numerically resolve the peaks even with moderate instrumental resolution. The acquisition times for Sm:YAG spectra ranged from 20 s to 10 min, depending upon the desired signal-to-noise ratio and upon how quickly pressure measurement were needed. Generally, the higher the *T* is, the longer the acquisition time.

During all experiments, the detection system was carefully calibrated using a neon emission lamp calibration standard with a 30 μm entrance slit. To ensure the highest possible precision of the calibration, the channel-to-frequency conversion for every Sm:YAG spectrum was done using an accompanying neon emission spectrum that was acquired immediately after the Sm:YAG spectrum. At the beginning of each run the zero-point *p*, namely, the apparent *p* value when real *p* is 1 bar, was calibrated using the spectra of Sm:YAG chips placed inside the sample chamber of an identical DAC without a pressure transmitting medium. Under proper optical alignment, the zero-point *p* values fall within ±0.3 GPa. The real *p* is obtained by subtracting the zero-point *p* from the apparent *p*. To keep the zero-point *p* constant, the optical path needed to be kept undisturbed during the experiment. The DAC, and thereby the Sm:YAG chips, tended to drift away from the laser spot, while *T* was changing or after *p* was adjusted. When this happened, the Sm:YAG chips were brought back into the laser spot without disturbing the optical path by shifting the furnace using an *x-y* translation holder that permitted positioning to within 10 μm.

III. RESULTS AND DISCUSSION

A. Pressure and temperature dependences of peak parameters for Y1 through Y10

The LANL spectra were used for establishing the *p* and *T* dependences of the Sm:YAG peaks. Typical spectra are shown in Fig. 1.

Most studies[10–12,14–17] have indicated that the peak shape of Y1 and Y2 can be well fitted by the standard Lorentzian function,

$$I(\omega)=\frac{I_0}{1+4(\omega-\omega_0)^2/\Gamma^2}, \tag{1}$$

where ω is the frequency, I_0 is the peak intensity or the height, ω_0 is the frequency of the peak position, and Γ is the full width at half maximum (FWHM). Lorentzian functions were used to represent all Y1 through Y10 peaks. The model profile was the sum of ten Lorentzian functions plus a linear background spanning from the valley left of Y1 (15 800 cm^{-1}) to the valley right of Y10 (17 200 cm^{-1}), and was least-squares fitted to the experimental spectra using a nonlinear least-squares algorithm.[22] The peak positions, widths and intensities for the Lorentzian functions, and the slope and the intercept for the linear background were independent variables (adjustable by the fitting routine), which are returned when the best fit is achieved.

For spectra taken at *T* below 400 °C, where every peak can be easily resolved and is distinguishable from the background, the fitting routine returned convergent and consistent results even if starting parameters for the fit were roughly estimated. For spectra taken at higher *T*, however, the peaks begin to broaden considerably, and attempting to fit with rough initial parameters tends to result in divergence. To get around the divergence problem, two measures were taken: (1) a width of a frequency range over which the profile is fitted was so selected and adjusted that the numerical stability can be achieved; and (2) the parameters obtained from the fitting the next lower temperature spectrum were used as the starting parameters. With these two measures the fitting procedure not only resulted in excellent fits between the model profiles and the measured spectra, as shown by Fig. 1, but also returned consistent results for peak parameters, as plotted versus *p* or *T* in Figs. 3–6. For the data plotted in Figs. 3–6, the uncertainties in the determinations of the peak positions for the strong peaks Y1–Y3, Y6, Y8, and Y10 were less than ±0.5 cm^{-1}, and for weak peaks Y4, Y5, Y7, and Y9 were within ±3 cm^{-1}; the uncertainties in *p* determinations were within ±0.07 GPa and in the *T* measurements were within ±2 °C. Note that because absolute intensity is irrelevant, only shown here is the relative intensity of Y*i* (*i* = 2–10) to Y1. It was observed that the pressure-induced

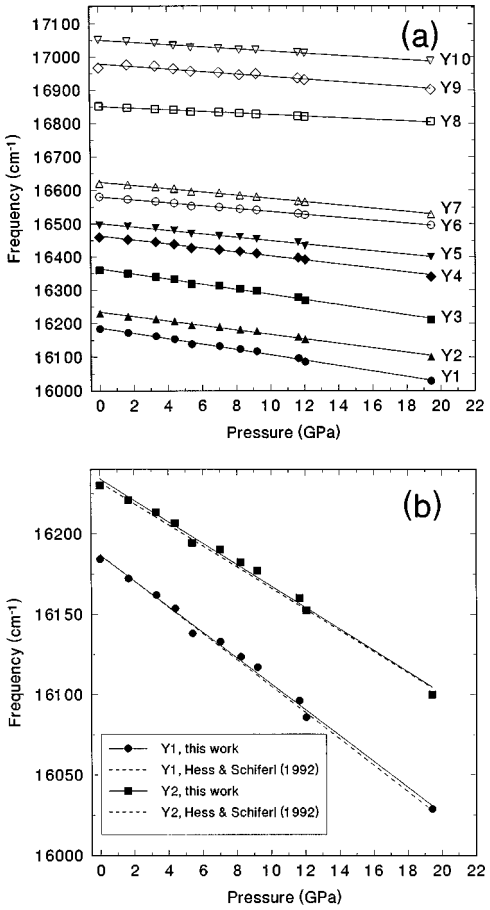

FIG. 3. Pressure dependence of the positions of the Sm:YAG Y1–Y10 fluorescence peaks at 20 °C. The symbols and the lines represent the experimental data and the best-fit functions, respectively. The present results for Y1 and Y2 and the results calculated from the empirical functions given by Hess and Schiferl (see Ref. 15) are plotted in (b) for comparison.

variations in peak widths and relative intensities were negligibly small under hydrostatic or nearly hydrostatic pressure below 20 GPa, in agreement with the previous observations.[12,14,15]

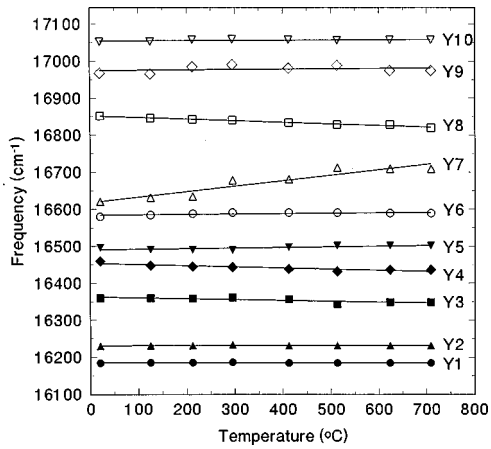

FIG. 4. Temperature dependence of the positions of the Sm:YAG Y1–Y10 fluorescence peaks at 1 bar. The symbols and the lines represent the experimental data and the best-fit functions, respectively.

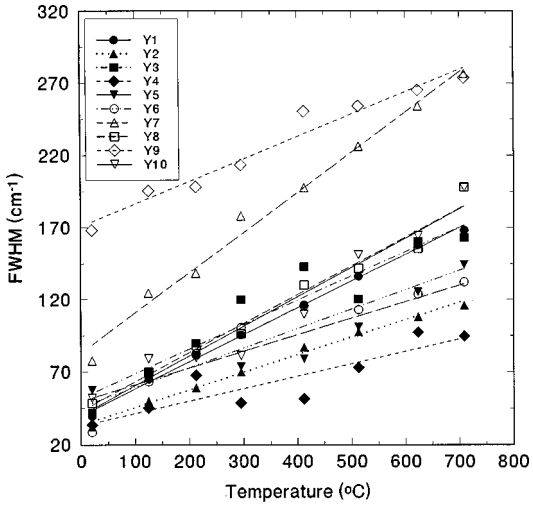

FIG. 5. Temperature dependence of the widths of the Sm:YAG fluorescence Y1–Y10 peaks at 1 bar. The symbols and the lines represent the experimental data and the best-fit functions, respectively.

Linear functions[12,14,15] and quadratic functions[13,17] have been used to describe the p dependence of the Y1 and Y2 positions. However, below 23 GPa, all data from different groups exhibit an excellent linearity versus p. For the present data that are below 20 GPa, we used linear functions to represent the relationship between the ith peak position, $\omega_{0,i}$ in cm^{-1}, and p in GPa,

$$\omega_{0,i}(p,\ 20\ ^\circ\mathrm{C}) = \alpha_i + \beta_i p. \tag{2}$$

These functions were found to fit to the present data very well. Likewise, linear functions for the relations between the peak positions and T (in °C),

$$\omega_{0,i}(1\ \mathrm{bar},\ \ T) = \delta_i + \epsilon_i T \tag{3}$$

and relations between the peak widths, Γ_i in cm^{-1}, and T

$$\Gamma_i(1\ \mathrm{bar},\ \ T) = \phi_i + \gamma_i T \tag{4}$$

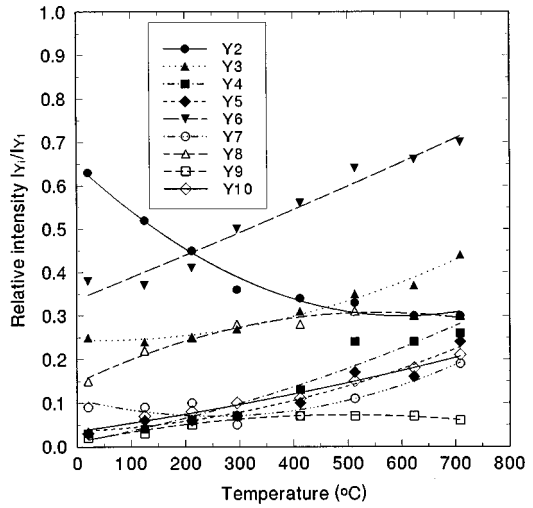

FIG. 6. Temperature dependence of the intensity ratio of Y2–Y10 to Y1 at 1 bar. The symbols and the lines represent the experimental data and the best-fit functions, respectively.

TABLE I. Fitting coefficient in Eq. (2).

Peak	α (cm^{-1})	Standard error	β(cm^{-1}/GPa)	Standard error
Y1	16186.8	1.8	−8.03	0.20
Y2	16234.3	1.9	−6.67	0.20
Y3	16363.9	2.0	−7.65	0.21
Y4	16463.7	1.8	−6.08	0.20
Y5	16500.9	1.8	−5.17	0.19
Y6	16580.3	0.8	−4.35	0.08
Y7	16624.4	1.1	−4.86	0.12
Y8	16851.0	0.6	−2.41	0.07
Y9	16979.2	2.9	−3.80	0.31
Y10	16051.0	1.2	−3.27	0.13

were also found to fit to the data very well. However, using linear functions to fit the data for relative intensities, h_i, led to very large scatters and very small correlation coefficients. For this reason, quadratic functions were used

$$h_i(1\ \text{bar},\ T) = \eta_i + \theta_i T + \kappa_i T^2. \tag{5}$$

The coefficients in Eqs. (2)–(5) were obtained by the least-squares regressions with p and T as the independent variables. The results are listed in Tables I–IV. The resulting functions are plotted as the lines in Figs. 3–6.

The LANL data used to establish T dependency were collected to 709 °C. At Harvard, data were collected up to 980 °C. Because the Harvard data have lower resolution and, above 900 °C, the data for width and relative intensity are not reliable, we did not combine the Harvard data into the LANL data when establishing Eqs. (2)–(5). Nevertheless, the extrapolations of Eqs. (2)–(5) agreed with the Harvard higher T data.

B. Pressure scales to 709 °C and higher temperature

The positions of Y1 and Y2 have been found to be virtually independent of T.[12,14,15] The present results (Fig. 4 and Table II) indicate that the positions of Y1 and Y2 have no significant T dependence. The irregular behavior of Y7 may arise from large uncertainty in the determination of its peak parameters, because it is rapidly hidden by the background as T increases.

Motivated by the observation that the Y1 and Y2 positions are T independent, Hess and Exarhos,[12] and Hess and Schiferl[14,15] proposed T-independent Y1 and Y2 p scales

TABLE II. Fitting coefficients in Eq. (3).

Peak	δ (cm^{-1})	Standard error	ϵ(cm^{-1}/°C)	Standard error
Y1	16185.0	0.5	-3.4×10^{-4}	1.23×10^{-3}
Y2	16230.9	0.7	1.17×10^{-3}	1.59×10^{-3}
Y3	16362.7	2.8	-2.220×10^{-2}	6.62×10^{-3}
Y4	16453.6	2.9	-3.098×10^{-2}	6.85×10^{-3}
Y5	16490.1	2.6	1.659×10^{-2}	5.96×10^{-3}
Y6	16583.7	1.8	1.132×10^{-2}	4.28×10^{-3}
Y7	16617.7	0.8	1.4796×10^{-1}	2.05×10^{-3}
Y8	16852.7	1.1	-4.359×10^{-2}	2.64×10^{-3}
Y9	16974.5	6.6	1.008×10^{-2}	1.54×10^{-3}
Y10	17054.2	1.4	6.029×10^{-2}	3.17×10^{-3}

TABLE III. Fitting coefficients in Eq. (4).

Peak	ϕ(cm^{-1})	Standard error	γ(cm^{-1}/°C)	Standard error
Y1	39.76	1.77	1.862×10^{-1}	4.1×10^{-3}
Y2	33.45	1.78	1.209×10^{-1}	4.1×10^{-3}
Y3	51.82	10.24	1.693×10^{-1}	2.4×10^{-3}
Y4	32.84	7.64	8.54×10^{-2}	1.8×10^{-3}
Y5	49.72	7.70	1.146×10^{-1}	1.8×10^{-3}
Y6	45.83	8.67	1.350×10^{-1}	2.0×10^{-3}
Y7	82.94	5.21	2.782×10^{-1}	1.2×10^{-3}
Y8	43.23	5.42	2.003×10^{-1}	1.3×10^{-3}
Y9	170.84	5.53	1.552×10^{-1}	1.3×10^{-3}
Y10	40.22	8.83	2.040×10^{-1}	2.1×10^{-3}

based on the p dependence of their positions. Without T correction, p can be determined based on the p dependence of the Y1 and Y2 positions over the p range of 0–25 GPa and the T range of -267–547 °C. Our data show that this T independence is maintained up to 850 °C and possibly higher.

Dropping T from the argument of $\omega_{0,i}$ in Eq. (2), and substituting the coefficients we obtained from the LANL data, Eq. (2) for Y1 and Y2 can be rewritten as

$$\omega_{0,1}(p) = 16186.8(1.8) - 8.026(0.196)p \tag{6}$$

and

$$\omega_{0,2}(p) = 16234.3(1.9) - 6.671(0.203)p, \tag{7}$$

where the numbers in the parentheses are the standard mean deviations. These are the Y1 and Y2 temperature-independent pressure scales we obtained and are using in the present study.

Several forms for the Y1 and Y2 scales have been published. It has been shown that all forms of these scales are consistent with the data from different sources, within experimental error. Therefore, we only compare our scale with one of them to check for consistency with all scales from the other sources. We choose the Y1 and Y2 scales given by Hess and Schiferl[15] because they correspond to an experimental condition closest to ours. Their scales, together with Eqs. (6) and (7), are plotted in Fig. 3(b). From Fig. 3(b), it can be seen that the difference between the two Y1 scales is quite small but increases with p, while the difference between the two Y2 scales is larger but decreases with p. The differences may be due to the differences in detection system calibrations and/or in the numbers of data points used for the fitting. Note that the Hess–Schiferl Y1 and Y2 scales shown in Fig. 3(b) were derived from a data set consisting of 57 data points. Nonetheless, the difference between the two Y1 scales is only 0.36 GPa at 20 GPa, resulting in an error of only ±2%. Because the Y1 peak is the strongest and most distinguishable peak, the Y1 scale is used for p determination. The exceedingly small difference between the two Y1 scales guarantees that the p values determined based on the present Y1 scale is consistent with those determined based on the Y1 scales established by others.

C. Pressure calibration using Y1 through Y10

To address the problem of a reliable p determination with overlapping peaks in the use of Sm:YAG, a fitting

TABLE IV. Fitting coefficients in Eq. (5).

Peak	η	Standard error	θ (1/°C)	Standard error	κ(1/°C^2)	Standard error
Y2/Y1	6.48×10^{-1}	1.7×10^{-2}	-1.157×10^{-3}	1.10×10^{-4}	9.96×10^{-7}	1.45×10^{-7}
Y3/Y1	2.44×10^{-1}	1.1×10^{-2}	-3.6×10^{-5}	7.1×10^{-5}	4.28×10^{-7}	9.3×10^{-8}
Y4/Y1	1.1×10^{-2}	2.9×10^{-2}	2.27×10^{-4}	1.87×10^{-4}	2.18×10^{-7}	2.45×10^{-7}
Y5/Y1	3.6×10^{-2}	1.9×10^{-2}	4.9×10^{-5}	1.22×10^{-4}	3.14×10^{-7}	1.60×10^{-7}
Y6/Y1	3.38×10^{-1}	3.0×10^{-2}	5.0×10^{-5}	1.91×10^{-4}	4.30×10^{-7}	2.51×10^{-7}
Y7/Y1	1.09×10^{-1}	1.8×10^{-2}	-3.1×10^{-5}	1.18×10^{-4}	5.97×10^{-7}	1.54×10^{-7}
Y8/Y1	1.47×10^{-1}	1.0×10^{-2}	5.78×10^{-4}	6.5×10^{-5}	5.21×10^{-7}	8.5×10^{-8}
Y9/Y1	1.1×10^{-2}	5×10^{-3}	2.48×10^{-4}	3.4×10^{-5}	2.50×10^{-7}	4.5×10^{-8}
Y10/Y1	3.6×10^{-2}	9×10^{-3}	1.74×10^{-4}	5.7×10^{-5}	9.5×10^{-8}	7.5×10^{-8}

method for the determination of the Y1 position needs to include Y1 through Y10. Three fitting routines that use Y1–Y10 are discussed here.

The fitting routines were designed following the common recipe: The model spectrum was built by summation of ten Lorentzian profiles (Y1 through Y10) plus a linear background with intercept a and slope b:

$$I(\omega)=\sum_{i=1}^{10}\frac{I_{0,1}h_i}{1+4(\omega-\omega_{0,i})^2/\Gamma_i^2}+a+b\omega, \tag{8}$$

where $I_{0,1}$ is the intensity of Y1, and the product of $I_{0,1}$ and h_i the relative intensity with $h_1\equiv1$, and Γ_i the FWHM for the ith peak. A nonlinear least-squares algorithm is used to minimize χ^2, which is defined as the sum of the weighed squared residuals between the model spectrum and the measured spectrum, with weighting factor set as the reciprocal square root of the intensity of the measured spectrum. The value of p corresponding to the minimized χ^2 is returned. There were 33 (not all independent) variables in the routines: p, the positions, $\omega_{0,i}$, widths, $\Gamma_{0,i}$, and relative intensities, $I_{0,1}h_i$, for Y1–Y10, and the intercept a and the slope b of the linear background. The main difference between each of the routines we tested lies in how to assign the peak parameters as either independent variables or dependent parameters. An ''independent variable'' is a quantity that varies freely in the fitting procedure. A ''dependent parameter'' is a quantity that is defined by p or T according to Eqs. (2)–(5). A dependent parameter can be a ''constant,'' e.g., a width or a relative intensity at a given T that is measured experimentally. It can also be a function of the independent variables, e.g., the Y1 position is a defined function of p.

Intuitively, all peak positions in a fit can be defined by a single p value according to Eq. (2), that is, all $\omega_{0,i}=\omega_{0,i}(p)$. Correspondingly, there are 23 independent variables; they are p, width Γ_i and intensity $I_{0,1}h_i$ of each of Y1–Y10, and intercept a and slope b for the linear background. In such a way, the p value returned by the fitting routine will be a value best fit to all ten peak positions. However, this procedure is problematic. First, in contrast to Y1 coefficients, the present coefficients in Eq. (2) for Y2 are not identical with the previous Y2 pressure scale; including Y2 as a pressure scale will introduce inconsistency. Second, even if Eq. (2) for all Y peaks could be used for p calibration without T correction, the larger uncertainties for the positions for the weak peaks appear likely to deteriorate the accuracy for the results that are obtained using solely Y1. As has already been pointed out,[16] p determination based on the Y2 scale is less accurate. Third, the positions of the other peaks are not as sensitive to p as that of Y1. Therefore, for all three routines we assigned the Y1 position as the only p-dependent parameter, with the positions of the other peaks assigned as independent variables. These p-independent (and also T-independent) variables were initialized with Eq. (2) and then were allowed to vary freely to achieve the best fit. Using this scheme, the p returned is only related to the Y1 position, and the Y2–Y10 peaks acted as pseudo ''background'' for the Y1 peak. The routines are outlined in Table V.

Routine 1. This routine has 32 independent variables: those outlined in Table V, and a and b for the linear background. Routine 1 worked satisfactorily up to ~550 °C. Examples of the p values given by Routine 1 are listed in Tables VI and VII, and examples of fitted profiles are shown together with the measured spectra in Fig. 7. Although Routine 1 can be used to achieve an excellent fit between a model profile and an experimental spectrum (i.e., the smallest χ^2), above ~550 °C it usually diverges, giving unrealistically large width values and negative intensity values for some of the weak peaks. This is due to the fact that at these T, the intensity-to-background ratios for most peaks except Y1 and Y6 are too low to be recognized by Routine 1.

Routine 2. To improve the stability of the fitting routine, and to have these weak peaks ''recognized,'' we assigned widths and relative intensities for all peaks, except Y1 and Y6, to be the constants that are determined solely by T according to Eqs. (4) and (5). By doing so, the numerical stability of the routine tended to be protected over the T range from 20 to 850 °C. However, the intensities and the widths for all peaks except Y1 and Y6 no longer corresponded to the best-fit values, because the peak widths and relative intensities may depend on specific instrumental and experimental conditions. In other words, the coefficients in Eqs. (4) and (5), which correspond to the instrumental and experimental conditions at LANL, are not necessarily identical to those for the spectra acquired at Harvard. This procedure, called Routine 2, uses 16 independent variables: those outlined in Table V, and a and b for the linear background. Fits to the measured spectra using Routine 2 are shown in Fig. 7. Although for the weak peaks the fit obtained using Routine 2 is not as good as the fit using Routine 1, the p values returned by both routines, as shown in Table VI, are still in

TABLE V. Descriptions of the pressure (p) determination methods using Y1-Y3 and using Y1–Y10.

Method	Description	Comment
Y1-Y3 fitting method	Obtain the Y1 position by fitting Y1, Y2, and Y3 without accounting for the neighboring peaks and calculate p from the Y1 scale	works up to ~550 °C tends to have larger uncertainty in determination of Y1 position above 450 °C
Routine 1	Obtain p from the Y1 scale by fitting Y1–Y10 simultaneously with the following scheme: p is an independent variable Position of Y1 is a function of p, Eq. (6) Positions of Y2-Y10 are independent variables All peak widths and intensities are independent variables	works up to ~550 °C tends to become divergent above 550 °C
Routine 2	Obtain p from the Y1 scale by fitting Y1-Y10 simultaneously with the following scheme: p is an independent variable Position of Y1 is a function of p, Eq. (6) Positions of Y2-Y10 are independent variables Width and intensities for peaks, except for Y1 and Y6, are the constants determined by T, Eq. (4)	works up to 850 °C or above, tends to give poor fits for those spectra with abnormal backgrounds in high frequency range
Routine 3	Obtain p from the Y1 scale by fitting Y1-Y10 simultaneously with the same scheme as Routine 2 except width of Y6 is determined by T, Eq. (4)	works up to 850 °C or above, also gives good fits for those spectra with abnormal backgrounds in high frequency range

good agreement. This indicates that essentially the Y1 position was hardly affected by the fixed widths and intensities of the weak peaks, largely because the Y1 peak was weighted much more heavily. When using Routine 2 to fit spectra obtained at T above 700 °C, however, it occasionally occurred that the returned positions of Y4, Y7, or Y9 were out of order with respect to the initial order of the peak positions. These peaks were completely hidden by the background in the experimental spectra, and these peaks always slip into the higher frequency range and hence ended up far away from Y1. Thus, this kind of behavior of these weak peaks does not affect the positions of Y1, Y2, Y3, and Y6, which are the most important peaks, and hence does not affect the p value. Occasionally, the background of a spectrum obtained at a T above ~800 °C was found to be irregularly high for frequency $>16\,600$ cm^{-1}, leading to either a poor fit or even divergence using Routine 2. This situation is shown in Fig. 7(c) (curve No. 3). This is the worst YAG spectrum that was acquired in our high-T and high-p semiconductor anneal experiments and was apparently caused by

TABLE VI. Comparison of Y1 positions $\omega_{0,1}(1)$, $\omega_{0,1}(2)$, and $\omega_{0,1}(3)$, and pressure values $p(1)$, $p(2)$, and $p(3)$ determined using Routines 1–3 for the room temperature spectra collected at LANL. The Y1 positions and p determined by routine 1 is used as the reference because routine 1 has been ''gauged'' by the ruby fluorescence measurements.

Routine 1		Routine 2		Routine 3	
$\omega_{0,1}(1)$ (cm^{-1})	$p(1)$ (GPa)	$\omega_{0,1}(2)$-$\omega_{0,1}(1)$	$p(2)$-$p(1)$	$\omega_{0,1}(3)$-$\omega_{0,1}(1)$	$p(3)$-$p(1)$
16183.9[a]	0.36	−0.2	0.03	−0.2	0.02
16172.6	1.78	−0.3	0.04	−0.3	0.03
16161.9	3.10	−0.2	0.02	−0.1	0.01
16153.7	4.13	−0.1	0.01	0.0	0.00
16138.1	6.06	0.0	0.01	0.0	0.00
16133.0	6.71	−0.1	0.01	0.0	0.01
16112.8	7.98	0.8	−0.10	0.8	−0.10
16117.1	8.69	0.1	−0.02	0.1	−0.02
16096.3	11.28	0.0	0.00	0.0	0.01
16085.8	12.58	−0.7	0.09	−0.7	0.09
16030.1	19.52	0.3	−0.01	0.2	0.00

[a]Data taken at 1 bar.

TABLE VII. Pressure (p) values determined from the Y1–Y3 fitting method and routines 1–3 at high temperature. The p values from the nitrogen vibron scale are also shown for some spectra. Δp_{Y1Y2} is the difference between the p value returned by the routine and the p value calculated from the Y2 position. All p and Δp_{Y1Y2} values are in GPa. The spectra with (*) were acquired at LANL The others were acquired at Harvard.

T(°C) with a spectrum[a]	Figure	Nitrogen vibron p	Y1–Y3 fitting		Routine 1		Routine 2		Routine 3	
			p	Δp_{Y1Y2}	p	Δp_{Y1Y2}	p	Δp_{Y1Y2}	p	Δp_{Y1Y2}
20±1	7(a)		5.18	0.17	5.20	0.17	4.97	0.26	4.97	0.28
144±2*		19.84	19.72	−0.03	19.15	−0.62	18.38	−0.67	18.38	−0.67
209±2*		18.76	18.96	−0.39	18.97	−0.24	18.28	−0.2	18.29	−0.21
298±2*		18.40	18.30	0.00	17.90	−0.60	17.40	0.50	17.96	−0.09
350±2			2.68	−0.28	2.57	0.40	2.56	0.02	2.53	0.14
414±2*	7(b)	17.77	16.90	0.60	16.80	0.60	16.80	0.00	16.87	−0.01
420±2			2.62	−0.13	2.47	−0.27	2.66	−0.05	2.63	0.39
575±3[a]			⋯	⋯	⋯	⋯	0.10	−0.31	0.09	−0.71
575±3	7(c)		⋯	⋯	⋯	⋯	3.45	−0.12	3.44	0.23
850±10[a]			⋯	⋯	⋯	⋯	0.28	0.43	0.32	−0.38
850±10	7(c)		⋯	⋯	⋯	⋯	5.31	−0.32	5.07	−0.52
850±10[b]	7(c)		⋯	⋯	⋯	⋯	⋯	⋯	2.62	−0.56

[a]Spectrum acquired at 1 bar.
[b]This spectrum has an abnormal high background at the high-frequency end.

an anneal duration too short to permit optimization of the Sm:YAG signal/background ratio.[4] Even though this is far from the typical situation, we need to address it to have a fitting routine that is robust, even for poor spectra.

Routine 3. To improve the goodness of fit for such spectra, we found it necessary to further refine Routine 2 by defining the width of Y6 by Eq. (4) while letting the relative intensity of Y6 remain as an independent variable. Using this method, we can avoid the divergence due to the abnormally high background in a few of the spectra obtained at $T > 800$ °C. This procedure is called routine 3. The number of independent variables is 15, just one less than Routine 2 has. This routine is outlined in Table V. Fits to the measured spectra using Routine 3 are shown in Fig. 7. The p values determined using Routine 3 are listed in Tables VI and VII.

Before we discuss reliability issues with the use of routines 1–3 at elevated T, we discuss the consistency among Routines 1–3 by comparing the Y1 peak frequencies and in turn the p values determined from these three routines at room T and p up to 20 GPa. Routine 1 is actually almost the same as the profile fitting routine that was used to derive the peak parameters given in Sec. III A. The only difference between them is that Routine 1 goes further to return a p value from the Y1 position (based on the Y1 position-p relationship), whereas the profile fitting routine in Sec. III A returns the Y1 position, with a p value given from the ruby measurement. The algorithm for Routine 1 can therefore be considered to have been calibrated by the ruby fluorescence measurements, and it is taken as the standard for the comparisons with Routines 2 and 3. Table VI shows comparison among frequencies for the Y1 positions and among the p values determined using Routines 1–3. From Table VI, it can be seen that, at room T, the p deviation given by comparing Routines 2 and 1, and Routines 3 and 1 are within 0.1 GPa over the p range from 0 to 19 GPa. This indicates that Routines 1–3 are all consistent with each other. For room-T determination of p, one can utilize any of them. However, Routine 3 is applicable over the widest T range. Additionally, because Routine 3 has the smallest number of independent variables, it takes the shortest computation time to return a result. Therefore, Routine 3 is the best choice.

D. Reliability

The reliability of Routines 1–3 at high T and p were assessed by comparing the p values determined from these routines with those obtained from the N_2 vibron pressure scale and from the Y1–Y3 fitting method of Hess and Schiferl. For T up to 414 °C, we were able to obtain simultaneously Sm:YAG spectra and the N_2 vibron Raman scattering spectra, and thus we can make a direct comparison of the p values determined from Routines 1–3 with those determined from the N_2 vibron scale. The results are listed in Table VII, together with the p values determined by the Y1–Y3 fitting method of Hess and Schiferl. From Table VII, it can be seen that the largest difference between the p values obtained using Routines 1–3 and the p values obtained from the N_2 vibron scale is about 1 GPa for simultaneous high-T and high-p conditions. Because the N_2 vibron scale is actually a tertiary p scale within an overall accuracy up to about ±1 GPa, discrepancy between the present methods and the N_2 vibron scale is not unreasonable.

At T above 414 °C, where we have no other pressure scales that can serve for direct comparison, we have devised three approaches that give us an idea of the reliability.

Approach No. 1: Considering that below 550 °C, a p value determined by the Y1–Y3 fitting method is in good agreement with a p value given by the ruby and the N_2 vibron scales, if Routines 1–3 give results consistent with those given by the Y1–Y3 fitting method for the same spectrum, then this is an indication that the accuracy of Routines 1–3 is comparable with the ruby and the N_2 vibron scales. As shown in Table VII, the difference among the p values obtained using different methods is typically within ±0.4 GPa. This discrepancy among Routines 1–3, which is due to the differences in the number and kind of parameter assignments made between the various routines, also falls within

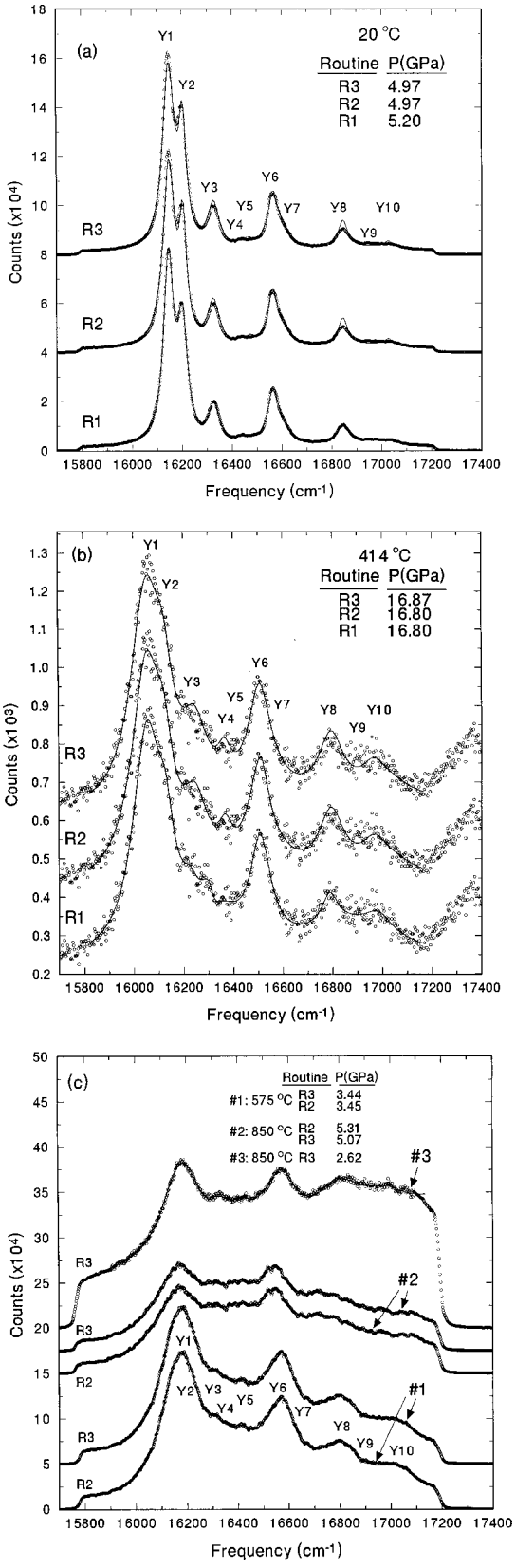

FIG. 7. Experimental spectra (circles) and fitted profiles (lines) using Routine 1 (R1), Routine 2 (R2), and Routine 3 (R3) for temperatures between 20 and 850 °C. Pairs of curves in (c) labeled with the same number show the same data overlaid on the output of different fitting routines. Successive spectra in (a) and (b) are offset by 4000 and 200, respectively. In (c), y intercept of each curve indicates offset. Note that curve No. 3 in (c) has an irregular background. When a fitting routine diverged, the result is not shown.

typical experimental errors in the p determination involving high T.

Approach No. 2: For a routine to be reliable, it must return a p value near 0 GPa for spectra known to be taken at atmospheric pressure (the only pressure we truly *know* at high T). We applied Routines 1–3 to the 1 bar spectra. That the p values returned for high T spectra were consistently no larger in magnitude than the typical largest random zero-point p value at 20 °C (~0.3 GPa) suggests that the routine is reliable over its applicable T range. Similar accuracy should be expected at higher pressures.

Approach No. 3. Spectra taken at high T (particularly those that must be taken quickly) may not be good enough for any fitting routine to work. The relative positions of Y1 and Y2 offer a check. Because Y2 is the immediate neighbor of Y1 and is relatively intense, if the Y2 position is terribly wrong then the Y1 position and hence the p value must be suspect. The figure of merit used to judge the reasonableness of the result of the fitting routine is the difference, Δp_{Y1Y2}, between the p value returned from the routine [i.e., calculated according to Eq. (6) from the fitted position of Y1] and the p value calculated according to Eq. (7) using the fitted position of Y2.[23] If this difference is not much larger than 0.5 GPa, then it suggests that routine is reliable. As indicated by Table VII, in general the absolute values for Δp_{Y1Y2} are reasonably small over the range 20–850 °C and comparable among different fitting methods (including the Y1–Y3 fitting method below 550 °C). However, the occasional appearance of a larger Δp_{Y1Y2} may signal that the quality of the spectrum is not very good (which happens often above ~850 °C) and that we have less confidence in the fitting. Note that as T increases, the decreasing intensity of Y2 makes larger Δp_{Y1Y2} values less of concern.

In summary, over the T range where the ruby and the N_2 vibron scales are applicable, p determined using Routines 1–3 based on the present Y1 scale can be considered to be as reliable and accurate as the ruby and N_2 vibron scales. At higher T, the Sm:YAG calibrant, in conjunction with present profiling fitting methods, can be used for p determination within an estimated uncertainty of 0.4 GPa. Because it gives good results over the largest T range, able to handle a spectrum with abnormal background, and takes the shortest computation time to return a result, Routine 3 is preferable for p determination.

IV. RECOMMENDATIONS

We recommend the use of ''Routine 3,'' in which p, peak positions of Y2–Y10, relative intensities of Y1 and Y6, and width of Y1 are all fitting parameters; the peak position of Y1 is a defined function of p; and widths of Y2–Y10 and relative intensities of Y2–Y5 and Y7–Y10 are defined functions of T. This routine is able to deal reliably with the most Sm:YAG spectra over the widest T range. Using this fitting routine, we can obtain (1) between 20 and 400 °C, p as accurate and reliable as with the ruby scale and the N_2 vibron scale; (2) over the T range from 400 to 850 °C, p values with

an estimated uncertainty of 0.4 GPa for spectra with small ($\leqslant$0.4 GPa) values of Δp_{Y1Y2} and with greater uncertainty for spectra with larger Δp_{Y1Y2} values.

ACKNOWLEDGMENTS

This work was supported by NSF-DMR-95-25907. Two of the authors (W.B.C. and S.D.T) were supported by the Harvard MRSEC under NSF-DMR-94-00396. Work at LANL was supported by the Division of Materials Sciences, DOE under Contract No. W-7405-ENG-36 with the University of California.

[1] L. C. Ming, M. H. Manghnani, J. Balogh, S. B. Qadri, E. F. Skelton, and J. C. Jamieson, J. Appl. Phys. **54**, 4390 (1983).
[2] D. Schiferl, J. F. Fritz, A. I. Katz, M. Schaefer, E. F. Skelton, S. B. Qadri, L. C. Ming and M. H. Manghnani, in *High-Pressure Research in Mineral Physics*, edited by M. H. Manghnani and Y. Syono (Terra Scientific Publishing Company, Tokyo, 1987), pp. 75–83.
[3] S. Mitha, M. J. Aziz, D. Schiferl, and D. B. Poker, Appl. Phys. Lett. **69**, 922 (1996).
[4] Y.-C. Zhao, M. J. Aziz, S. Mitha, and D. Schiferl, Mater. Res. Soc. Symp. Proc. **442**, 305 (1997).
[5] J. D. Barnett, S. Block, and G. J. Piermarini, Rev. Sci. Instrum. **44**, 1 (1973).
[6] G. J. Piermarini and S. Block, Rev. Sci. Instrum. **46**, 973 (1975).
[7] H. K. Mao, P. M. Bell, J. W. Shaner, and D. J. Steinberg, J. Appl. Phys. **49**, 3276 (1978)
[8] H. Arashi and M. Ishigame, Jpn. J. Appl. Phys., Part 1 **21**, 1647 (1982).
[9] A. Lacam and C. Chateau, J. Appl. Phys. **66**, 366 (1989).
[10] B. Lorenz, Y. R. Shen, and W. B. Holzapfel, High Press. Res. **12**, 91 (1994).
[11] S. C. Schmidt, D. Schiferl, A. S. Zinn, D. D. Ragan, and D. S. Moore, J. Appl. Phys. **69**, 2793 (1991).
[12] N. J. Hess and G. J. Exarhos, High Press. Res. **2**, 57 (1989).
[13] Q. Bi, J. M. Brown, and Y. Sato-Sorensen, J. Appl. Phys. **68**, 5357 (1990).
[14] N. J. Hess and D. Schiferl, J. Appl. Phys. **68**, 1953 (1990).
[15] N. J. Hess and D. Schiferl, J. Appl. Phys. **71**, 2082 (1992).
[16] J. Liu and Y. Vohra, Appl. Phys. Lett. **64**, 3386 (1994) Note that the peak labeled as Y4 by Liu and Vohra is the Y6 peak in the present paper.
[17] H. Yusa, T. Yagi, and H. Arashi, J. Appl. Phys. **75**, 1463 (1994).
[18] D. Schiferl, M. Nicol, J. M. Zaug, S. K. Sharma, T. F. Cooney, S.-Y. Wang, T. R. Anthony, and J. Fleischer, J. Appl. Phys. **82**, 3256 (1997). While it may appear that the Sm:YAG scale could be calibrated against the diamond Raman scale, the diamond Raman scale itself has not been calibrated at simultaneous high *p* and high *T*.
[19] J. L. Bates and J. E. Garnier, Commun. Am. Ceram. Soc. C-138 (1981).
[20] D. Schiferl, S. K. Sharma, T. F. Cooney, S.-Y. Wang, and K. Mohanan, Rev. Sci. Instrum. **64**, 2821 (1993).
[21] A. S. Zinn, D. Schiferl, and M. F. Nicol, J. Chem. Phys. **87**, 1267 (1987).
[22] The routines used here for spectrum analysis and pressure determination are written in GENPLOT macros. The GENPLOT package is provided by Computer Graphic Service, Lansing, NY.
[23] This is the only place where we use the position of a peak other than Y1 to extract a *p* value, and only as a check on the value extracted from the position of Y1.